Available online at www.sciencedirect.com

SciVerse ScienceDirect

Scripta Materialia 67 (2012) 37–40

Scripta MATERIALIA

www.elsevier.com/locate/scriptamat

Reasons for incomplete shape recovery in polycrystalline Fe–Mn–Si shape memory alloys

Xiaohua Min,[a,*] Takahiro Sawaguchi,[a] Xin Zhang[c] and Kaneaki Tsuzaki[a,b]

[a]*National Institute for Materials Science, Tsukuba, Ibaraki 305-0047, Japan*
[b]*Graduate School of Pure and Applied Sciences, University of Tsukuba, Ibaraki 305-0047, Japan*
[c]*Key Laboratory for Anisotropy and Texture of Materials, Northeastern University, Shenyang 110004, PR China*

Received 25 January 2012; revised 13 March 2012; accepted 14 March 2012
Available online 20 March 2012

Quantitative surface relief analysis proved that the incomplete shape recovery of a polycrystalline Fe–28Mn–6Si–5Cr alloy was not caused by slip deformation on loading but by irreversible phase transformation on heating, under given conditions ($[5\bar{4}\bar{1}]$ tensile axis, 5.9% strain). The observed area showed a higher recovery strain than the macroscopic recovery strain, implying inherently high reversibility. However, the value was significantly lower than that of a single crystal, due to the geometric constraint from surrounding grains, which reflected different transformation dislocations between forward and reverse transformations.

Keywords: Fe–Mn–Si shape memory alloy; Martensitic phase transformation; Polycrystal; Crystallography; Atomic force microscopy

Fe–Mn–Si shape memory alloys, which undergo the martensitic transformation from γ (face-centered cubic, fcc) austenite to ε (hexagonal close packed, hcp) martensite, have been studied extensively over the past several decades. The shape memory effect was first observed in a single crystal Fe–30Mn–1Si (mass%) alloy [1], and then in polycrystalline Fe–(30–32)Mn–6Si alloys [2]. Various alloy compositions [3] and processes [4] were developed, and Cr- and/or Ni-bearing alloys, e.g. Fe–28Mn–6Si–5Cr, with a good combination of mechanical properties and corrosion resistance are now being used for pipe joints and rail couplings [5,6].

The shape memory property depends on the orientation of the γ grain based on the Schmid factor (η) of Shockley partial dislocation, which is the transformation dislocation in the $\gamma \rightarrow \varepsilon$ transformation. A single crystal Fe–Mn–Si alloy exhibits a shape recovery strain of 8% when tensile deformation occurs in the $\langle 4\,1\,4\rangle$ direction ($\eta = 0.5$), while the recovery strain in the $\langle 0\,0\,1\rangle$ direction ($\eta = 0.236$) is only one-fifth of that in the $\langle 4\,1\,4\rangle$ direction [1,7]. Due to the random orientation of grains, the polycrystalline Fe–Mn–Si alloys show lower recovery strains ranging from 2 to 4%.

The poor shape memory properties of polycrystalline alloys may not be caused only from the average of grains with various orientations. The inter-granular constraints may also have an effect on the macroscopic properties. The incomplete shape recovery is caused by either the concurrent dislocation glide or the irreversibility of phase transformation [8,9]. From these points of view, we evaluate the contributions from the two deformation modes on loading and the reversibility of phase transformation on subsequent heating, in a grain with a tensile axis close to the $\langle 4\,1\,4\rangle$ direction in the polycrystalline Fe–Mn–Si shape memory alloy. The results are compared to those reported for the $\langle 4\,1\,4\rangle$ single crystal, and the possible reasons for the incomplete shape recovery are discussed.

A conventional polycrystalline Fe–28Mn–6Si–5Cr shape memory alloy was prepared by vacuum induction melting, and subsequent hot forging, hot rolling, solution treatment and water quenching. The forward and reverse martensitic transformation start temperatures, M_s and A_s, were 270 and 330 K, respectively. The tensile test (gauge dimension: 30 (l) × 4 (w) × 1 (t) mm, initial strain rate: 1.7×10^{-4} s^{-1}) was carried out at ambient temperature and the recovery heating was made at 623 K. The pre-strain and recovery strain measured by the gauge length were 5.9 and 1.9%, respectively.

The surface relief formed by straining on the pre-polished surface and its change after heating were analyzed

* Corresponding author. Tel.: +81 29 859 2529; fax: +81 29 859 2101; e-mail addresses: MIN.Xiaohua@nims.go.jp; minxiaohua2008@yahoo.com.cn

1359-6462/$ - see front matter © 2012 Acta Materialia Inc. Published by Elsevier Ltd. All rights reserved.
http://dx.doi.org/10.1016/j.scriptamat.2012.03.015

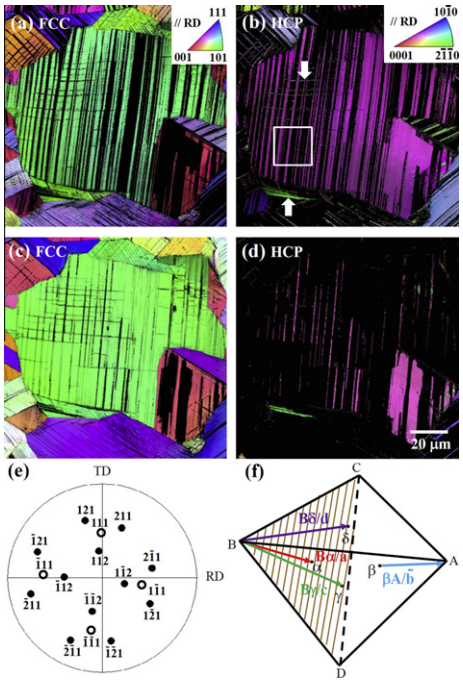

Figure 1. Maps combining inverse pole figure and image quality: (a and b) for the tensile strained specimen; (c and d) for the subsequently heated specimen; (e) the corresponding stereogram; and (f) a Thompson tetrahedron with four operative shear systems. (a and c) γ-Phase map; (b and d) ε-phase map. The tensile axis parallel to the RD is the horizontal direction.

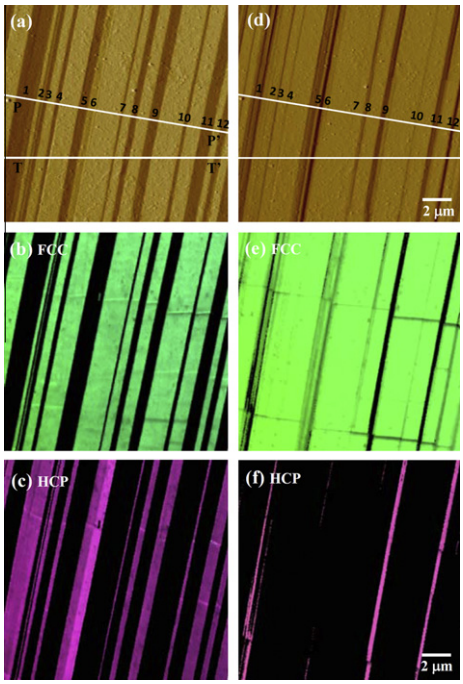

Figure 2. AFM images and maps combining inverse pole figure and image quality: (a–c) for the tensile strained specimen; (d–f) for the subsequently heated specimen. (a and d) Differential image of surface relief; (b and e) γ-phase map; (c and f) ε-phase map. The tensile axis parallel to the RD is the horizontal direction.

by atomic force microscopy (AFM; Keyence VN-8000, contacting mode). This method was previously applied to the same alloy by Liu et al. [10] to discuss the reversibility of phase transformation. In this study, the same area was further subjected to electron backscattering diffraction (EBSD; Carl-Zeiss LEO-1550) for determination of crystallographic orientation and phase identification. Note that the average confidence index values are higher than 0.6 even with the presence of surface relief.

A nearly ⟨4 1 4⟩ oriented grain was selected from the EBSD (step size: 0.3 μm) and shown in the central part of Figure 1. The grain is ~100 μm and the crystallographic orientation is determined to be ND//[3 $\bar{1}$ 19] and RD//[5 4 $\bar{1}$]. The RD parallel to the tensile axis is deviated 6° from the [4 4 $\bar{1}$] direction toward the inside of stereographic triangle of [1 0 0]–[1 $\bar{1}$ 0]–[1 $\bar{1}$ $\bar{1}$]. The crystallographic orientation is visualized in the stereogram and the Thompson tetrahedron in Figure 1e and f, respectively. Only four shear systems among the 12 possible shear systems, i.e. Bα[1 $\bar{1}$ $\bar{2}$]/a($\bar{1}$ 1 $\bar{1}$), βA[1 $\bar{1}$ 2]/b($\bar{1}$ 1 1), Bγ[1 $\bar{2}$ $\bar{1}$]/c($\bar{1}$ $\bar{1}$ 1) and Bδ[2 $\bar{1}$ $\bar{1}$]/d(1 1 1), are operative under tensile loading for this orientation, and the shear system of the parallel ε plates with pink color in Figure 1b[1] is deduced as the Bα/a with the highest Schmid factor (η = 0.494) and theoretically calculated tilt angle (θ = –8.9°) [11]. Most of the ε martensite plates disappeared after heating; however, some of the plates still remained (Fig. 1d). Note that thin ε plates undetectable under the EBSD may still exist. The area outlined in white in Figure 1b was used for a further study.

[1] For interpretation of color in Fig. 1, the reader is referred to the web version of this article.

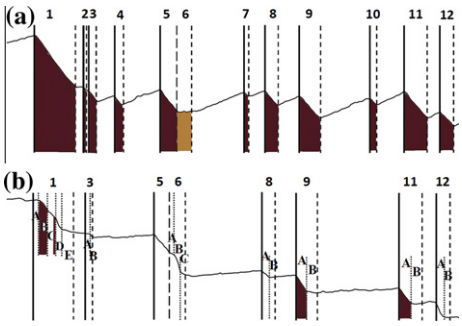

Figure 3. Surface relieves (a) for the tensile strained specimen and (b) for the subsequently heated specimen obtained from the AFM images by cross-sectional analysis along the white line P–P′ perpendicular to the surface trace of the plates (Fig. 2). The detected ε plates under the EBSD are hatched.

Figure 2 shows the differential AFM images, γ-phase and ε-phase maps (step size: 0.05 μm) taken after deformation (a–c), and those taken after heating (d–f), from the outlined area in Figure 1b. The brown colored bands in the AFM image, representing the surface relief by shear displacement, are in good agreement with the ε plates observed under the EBSD before heating. After heating, most of the ε plates disappeared, leaving several thin plates as shown in the ε-phase map; however, the AFM image still shows a significant number of plates (Fig. 2d).

Two kinds of surface profiling analyzes are made: one is the local strain analysis (LSA) in the cross-section along the white line T–T′ parallel to the tensile direction in Figure 2a, and the other is the surface tilt angle